



INTERNATIONAL INSTITUTE OF WELDING

A world of joining experience

Delegation of Austria

XIII-WG2-136-13

Numerical simulation loop to investigate the local fatigue behaviour of welded and HFMI-treated joints

David Simunek, Martin Leitner and Michael Stoschka

Montanuniversität Leoben, Chair of Mechanical Engineering, Austria

Abstract

High frequency mechanical impact (HFMI) for fatigue strength improvement of welded joints is a common post-treatment technique in industrial applications. Compressive residual stresses, a reduced notch effect at the weld toe, and additionally a local work hardening of the material are the main influences increasing fatigue life. Recent research results concerning the fatigue assessment of high frequency mechanical impact (HFMI)-improved fillet welds by local approaches are presented in [1].

In this work a simulation loop is set-up including structural welding simulation, numerical computation of the HFMI-process, and finally, an estimation of the local fatigue behaviour. To investigate the acting transient forces during post-treatment, strain gauge measurements at the hardened pin are performed and further on set as input parameters for the simulation. Micrographs of welded and HFMI-treated specimens are analysed to determine geometrical and microstructural modifications during manufacturing.

A structural weld simulation based on experimental data is built-up to investigate residual stress and strain conditions due to the welding process. The resulting local microstructural dependent material behaviour and residual stresses are used for the numerical simulation of the HFMI-process. X-ray measurements of the local residual stress state at welded and HFMI-treated specimens are performed to compare numerical and experimental results. Finally, a numerical estimation of the local fatigue behaviour by the finite element post-processor FEMFAT® is executed to compare the benefit by HFMI-treatment. The introduced simulation loop offers the opportunity to investigate and optimize local influences of different weld process and HFMI-treatment parameters in regard to fatigue.

Keywords: High frequency mechanical impact (HFMI), Fatigue strength improvement, Closed simulation loop, Structural welding simulation, Local fatigue assessment

1 Introduction

The welding process causes distortion and residual stresses in the structure. The acting operational loads and the generally tensile weld residual stresses are superimposed. The effective maximum local stress in the structure is significantly higher (Fig. 1). Furthermore the weld toe topography represents a sharp notch and small initial cracks are often observed in the weld toe region.

All these phenomena causes a reduced fatigue life time of welded structures. HFMI post-treatment is a statistically proven method to increase fatigue life of welded joints significantly. Thereby a hardened metal pin is hammering on the weld toe with high frequency and causes local plastic deformation in this area. The weld toe geometry is round out and reduces the notch concentration, compressive residual stresses are induced, the top surface is hardened and welding induced small cracks on surface are closed by the treatment.

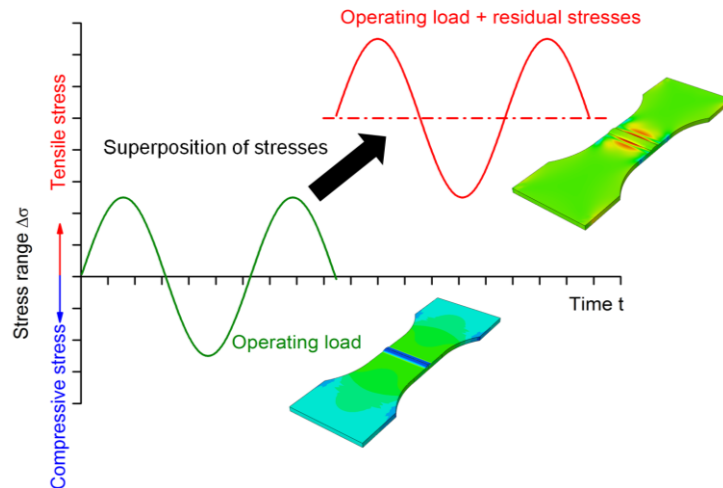


Fig. 1: Superposition of tensile weld residual stresses [2]

The change in local geometry and material properties due to welding and HFMI-treatment changes the geometric and metallurgical notch at the most-stressed weld toe. In this work numerical investigations based on experimental data are made to build up a closed three-dimensional simulation loop and to determine the change in local lifetime of a butt joint specimen.

2 Objectives

The aim of the work is to built-up a simulation loop including structural thermo-mechanical coupled weld simulation, transfer of the transient results into a structural finite element code, numerical investigation of the HFMI process and a finally a comparable computation of the local fatigue behaviour. Input parameters for the simulation of the HFMI-treatment are determined by experimental investigations. Fig. 2 depicts a flowchart of the characteristic process steps.

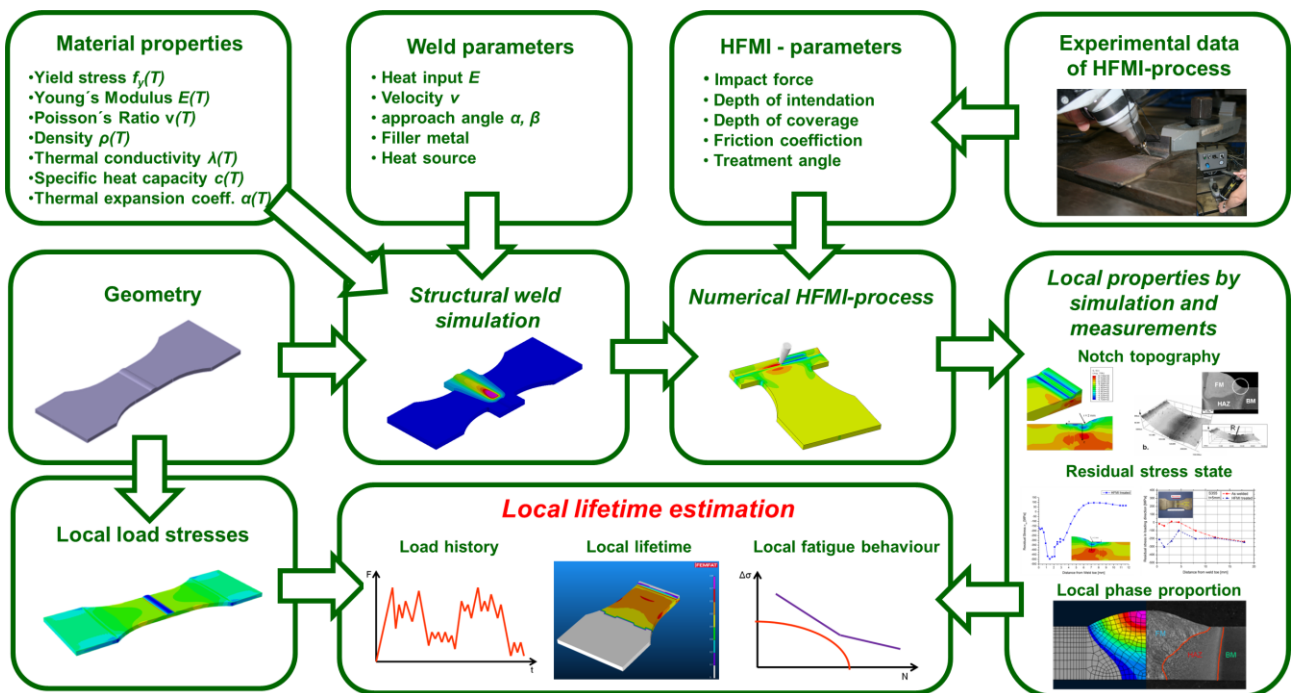


Fig. 2: Simulation loop and durability analysis of HFMI post-treated joints

3 Experimental investigations

The benefit of fatigue strength due to high frequency mechanical impact (HFMI) treatment of welded joints depends on a reduction of residual tensile stresses and geometric notch effects plus hardening of the hammered surface layer. Fatigue tests at a tumescent ration of $R=0.1$ have been made to investigate the factor of improvement on butt joint and T-joint specimens.

In Fig. 3 the nominal S/N-curve of HFMI-treated specimens is compared to as-welded joints and the base material of a common construction steel S355. The results are part of an extensive test programme for HFMI-treated joints focussing on the effect of high-strength steels and different joint geometries [3]. The IIW-recommendation [4] defines a nominal stress range of 90 MPa for the structural detail of a butt joint with ground flush to plane root surface. In case of very high manufacturing quality including grinding of the root surface and lateral plate surfaces, a benign thinness factor can be applied [5]. This leads to a non-conservative increase of the IIW-recommended FAT-class for the as-welded joint up to $FAT125$. The IIW-recommended [4] bonus factor for the HFMI post-treatment of steel with a yield strength of 355 MPa is a benefit factor of 1.5 . As the weld toe notch factor of the investigated thin-walled butt joint is comparable low, the benefit in improvement due to the HFMI-treatment is quite small. The fatigue stress range at two million cycles increases from $FAT185$ up to $FAT220$ for the butt joint, leading to an increase of 18% . Nevertheless, if the experimentally determined fatigue strength is compared to a value of $FAT125$ as gained by the IIW-recommended structural detail enhanced by the benign thinness factor, the improvement due to HFMI-treatment is evaluated as 76% . As shown in Fig. 3, the fatigue behaviour of the welded and HFMI-treated joint is close the base material strength of $FAT250$.

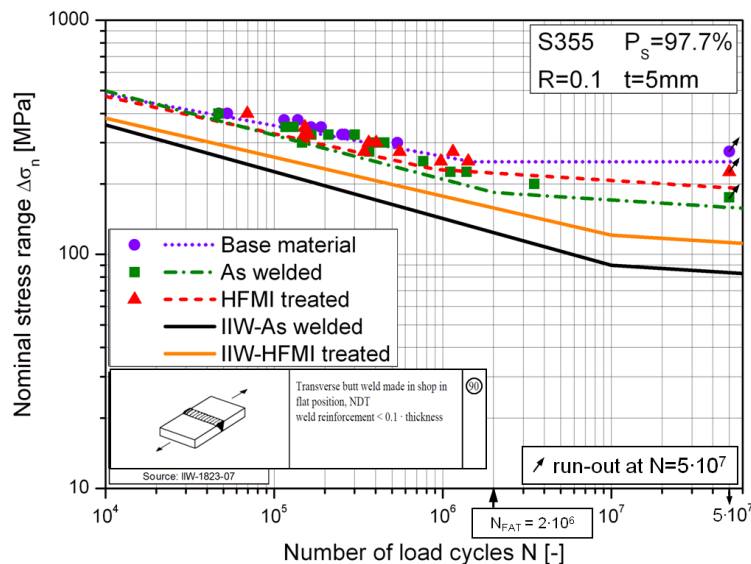


Fig. 3: Nominal S/N-curve of butt joints for S355 [3]

Based on experimental fatigue results, the difference between base material, as-welded and HFMI-treated condition is quite small but recognizable in the finite life region. In the high-cycle fatigue region, the improvement in fatigue strength is more pronounced.

3.1 Residual stress measurements

X-Ray diffraction measurements are performed to determine the residual stresses in the structures after welding and HFMI-treatment. The evaluation is based on Bragg's Law. Starting point of the measurement is the weld toe. Two different paths were analysed, first perpendicular to the joint and in depth at the weld toe. The results are shown in Fig. 4. Due to manufacturing of the metal sheets by thermo-mechanical controlled rolling threads, compressive residual stresses of about 200 MPa are induced in the metal plates. This manufacturing induced pre-stressing influences the condition of the residual stress state outside the molten zone, especially in the surface layer of the plate. The HFMI-treatment changes the residual stress state towards compressive stresses by about 300 MPa , which corresponds to the yield strength of the material.

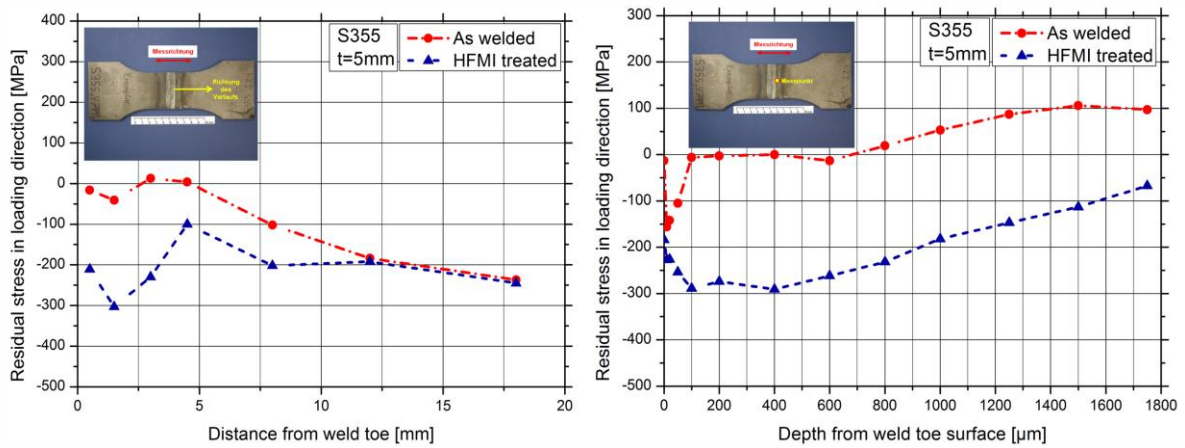


Fig. 4: Residual stress distribution along surface and in depth [6]

3.2 Impact force measurement

The high-frequency pneumatic impact tool PIT was used for the HFMI post-treatment. The tool requires an air pressure of $p=6 \text{ bar}$, the operating frequency is 90 Hz and the pin is moved along the weld with a speed of $v=20 \text{ to } 30 \text{ cm/min}$ to obtain a high quality of treatment at the weld toe.

The power of the hardened pin impact is essential for the plastic deformations at the HFMI-treated area. Therefore a strain gauge was added onto the surface of a hardened pin to determine the transient impact forces during the post treatment. In this investigation an 80 mm long pin with a tip radius $R=2 \text{ mm}$ is used. The strain gauge is applied on the cylindrical shaft of the tool pin, see Fig. 5. One strain gauge in quarter bridge connection measures the axial force. The evaluation of the dynamic impact force measurement matched the transient movement of the pin. Each compressive peak intends an impact of the pin onto the specimen surface.



Fig. 5: Strain gauge measurement at hardened pin [6]

The results of strain gauge measurements by manual operation of the PIT-tool are shown in Fig. 6. Due to a high logging frequency of at least 1.2 kHz the necessary time steps for evaluation of the transient impact force are kept. The impact forces scatter because of manual usage of the device. The evaluated compressive force peaks are between 1 kN and 2.5 kN . Therefore the device was clamped between two jaws and the pin impact on an additional restraint steel plate. The scatter band of the transient forces in Fig. 7 reduces significantly leading to compressive force values between 1.5 kN and 2.25 kN .

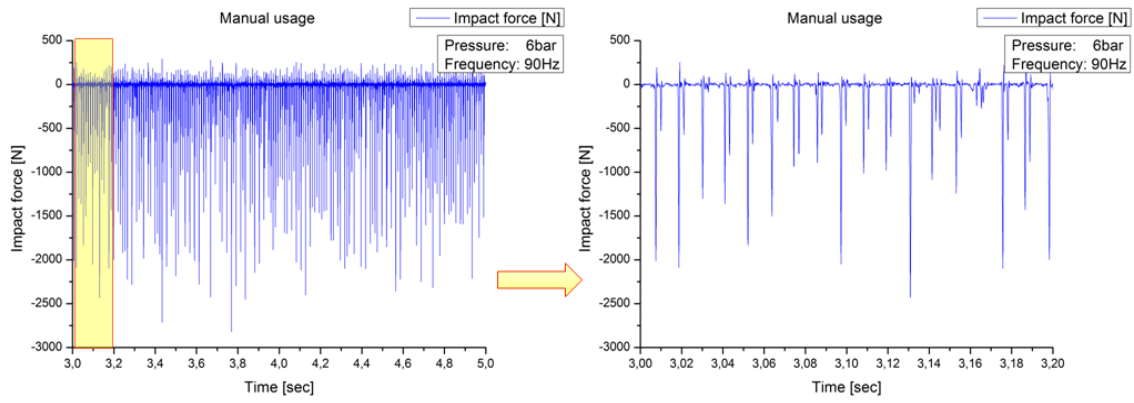


Fig. 6: Transient acting forces by manual operation [6]

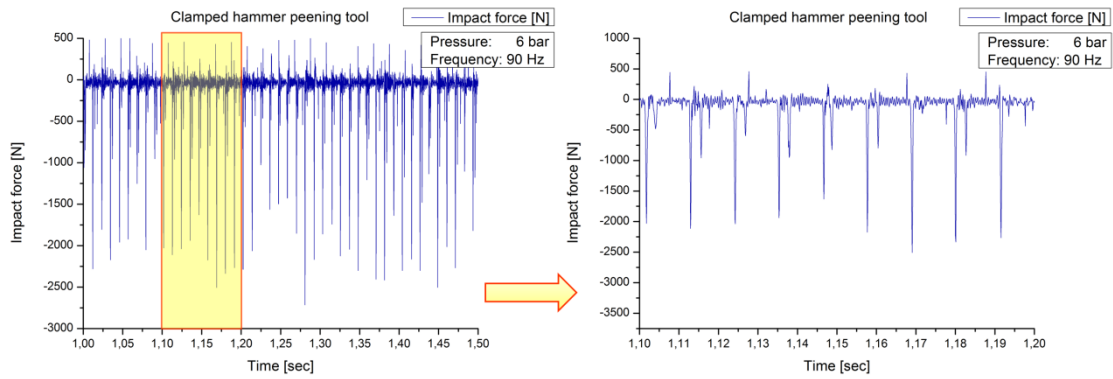


Fig. 7: Transient acting forces by operation with clamped tool [6]

The mean value of the transient impact force is nearly the same for both conditions. A quality criterion for the PIT-treatment is a sufficient overlapping of the individual impacts by optical inspection. To ensure that each impact has enough power in regard to plastic deformation of the work piece, a PIT-Almen test is recommended to experimentally validate the power of the HFMI-treatment before treating the weld toe. Thereby a small steel plate is fixed into a clamping device and peened along two lines until the impacted area shows a smooth and rounded surface. After unclamping of the metal sheet, the inherent concave deformation due to the HFMI-treatment of the plate can be measured.

4 Numerical investigations

4.1 Structural weld simulation

First, a half symmetrical butt joint model was built up according to the welded specimen geometry of the fatigue test samples. Along the weld line two run out areas are added, see Fig. 8. This inhomogeneous start and stop areas of the weld seam are therefore not within the test specimen cross section. The HFMI-treatment is applied onto the whole weld toe length; these overlapping lateral surfaces are cut-off after the treatment. These numerical model steps are identical to the manufacturing process.

The shape of the joint is based on micrographs of metallographic sections, the applied weld toe radius possesses a value $r=0.3\text{ mm}$ which was gained by non-destructive laser-confocal measurement of the weld toe region. The length of the weld seam of one specimen is 90 mm including the run out plates. The input parameters of the structural weld simulation, energy input per unit length $E=8.0\text{ kJ/cm}$ and welding speed $v=60.0\text{ cm/min}$, are identical to the real process.

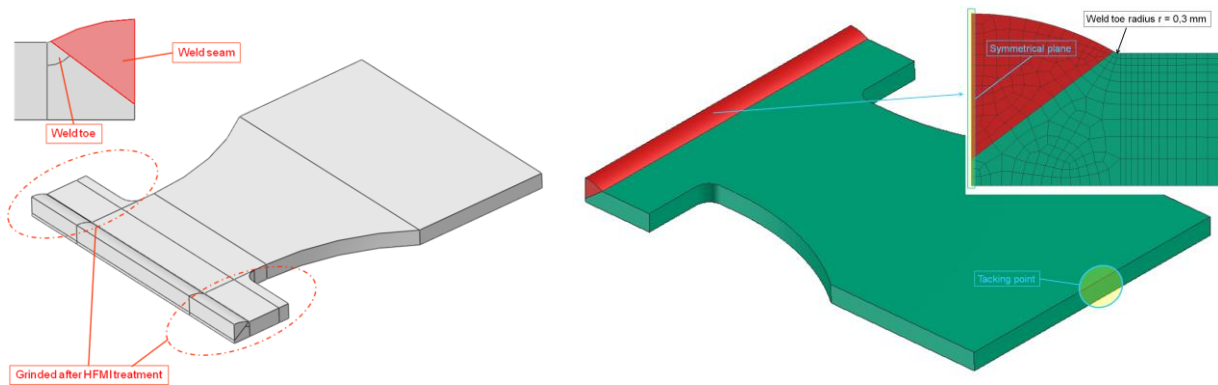


Fig. 8: Half-symmetrical model for structural welding simulation [6]

The weld toe area requires a fine mesh for the plastic deformations of the further following HFMI post-treatment. Accordingly to the manufacturing process, the specimens in Fig. 8 are clamped with tacking points at the end of the plates and unclamped after final-cooling.

The thermo-mechanical coupled structural weld simulation using Sysweld® calculates first the transient temperature distribution including the time-temperature dependent phase transformations. The heat-input is automatically calibrated to the given heat-input per unit length. The shape and length of the molten zone are adjusted to observations of the real weld process. After the thermo-metallurgical run the mechanical computation including the contact behaviour to the padding support and tacking points is solved. The unclamping occurs after final cool-down of the welded plate. Fig. 9 depicts the temperature distribution during welding.

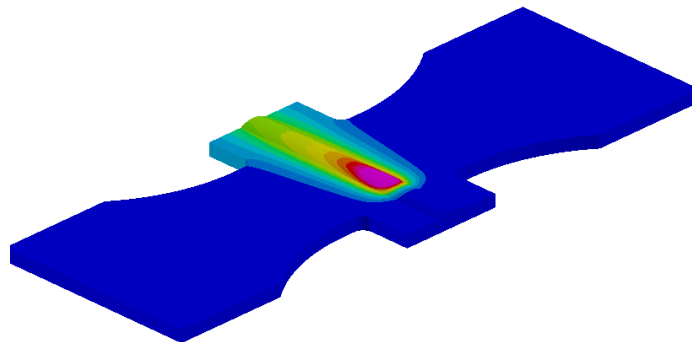


Fig. 9: Temperature distribution during welding process [3]

An image series in Fig. 10 shows the temporary change in molten zone in the cross section of the specimen during welding. The blue coloured areas are slightly above the melting temperature. The whole thickness of the plate melts up leading to a full penetrated butt-joint.

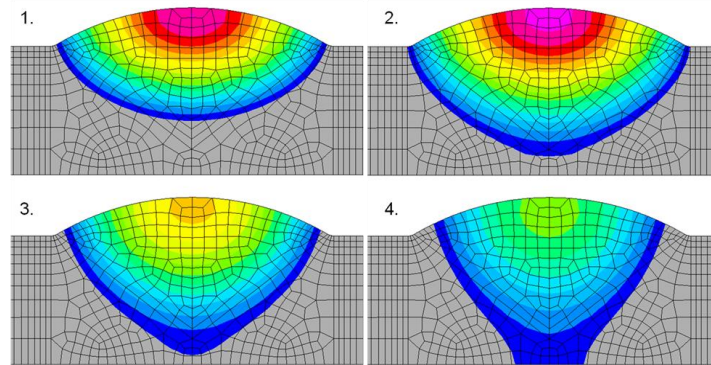


Fig. 10: Chronology of development of molten zones during welding [6]

The envelope of the molten area is compared with a metallographic section in Fig. 11. The three main areas – base metal BM, heat-affected-zone HAZ and molten filler metal FM - are labelled in the micrograph. The shape of the numerical weld seam is in good accordance to the real weld process.

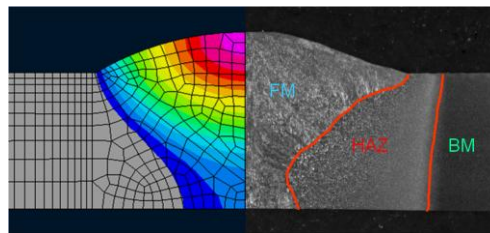


Fig. 11: Comparison of welding simulation with micrograph [6]

The residual stresses σ_{xx} perpendicular to the weld seam are shown in Fig. 12. The maximum values are located in the centre of the weld toe. During dynamic loading, the tensile residual stresses are superimposed with the tumescent load and the notched weld toe region causes fatigue failure at this region. Beside the weld toe region, the root surface is also loaded with tensile residual stresses.

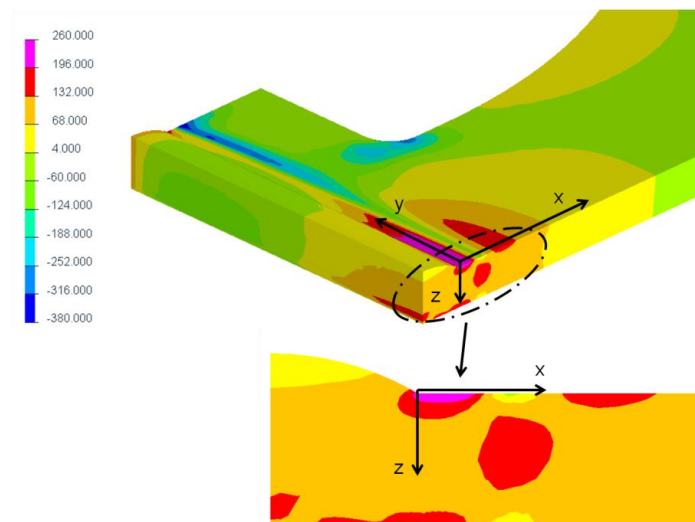


Fig. 12: Residual stress distribution after structural welding simulation [6]

The charts of the transversal residual stress distribution are shown in Fig. 13. At the weld toe, a tensile residual stress peak of about 275 MPa is observable. Defined by the phase-dependent properties of the material database, compressive residual stresses due to the martensitic solid-state transformation are introduced. This leads to a significant decrease of the simulated tensile residual stresses. The development of this compressive peak is mainly influenced by the used material database for the thermo-metallurgical calculation.

Several databases for the same structural steel are compared in [7] demonstrating that even slight differences in the material database influence the residual stress result in a major way. The residual tensile stress distribution into plate depth generally decreases, but increases again after half of the plate thickness again towards the root surface.

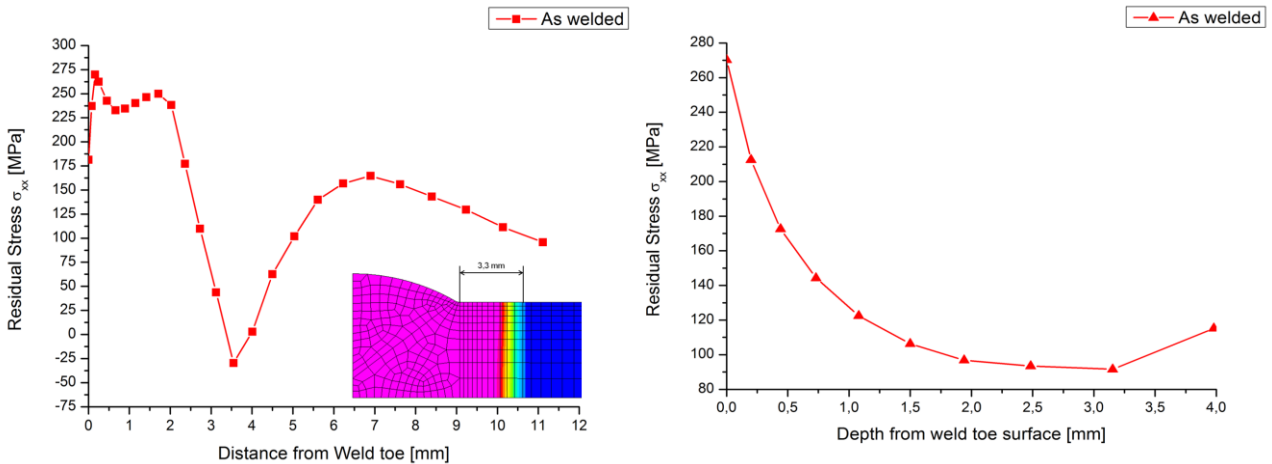


Fig. 13: Charts of simulated residual transversal stress distribution [6]

This three-dimensional residual stress distribution and the local change in material properties is further on used as input deck to the subsequent simulation of the HFMI-treatment process.

4.2 HFMI-treatment

4.2.1 Preliminary investigations

In these preliminary investigations different hardening laws of material, depth and overlapping of indentations are analyzed. First, the required overlaps according to the pin's top diameter and the mesh size in the weld toe are investigated to achieve a smooth peened surface. Therefore a simulation model consisting of a rigid pin surface acting on a single sheet metal plate is investigated in Fig. 14. The mesh spacing is very fine at the impact zone and coarsens towards the outer region. In the contact area, an element length of about fifty microns is modelled.

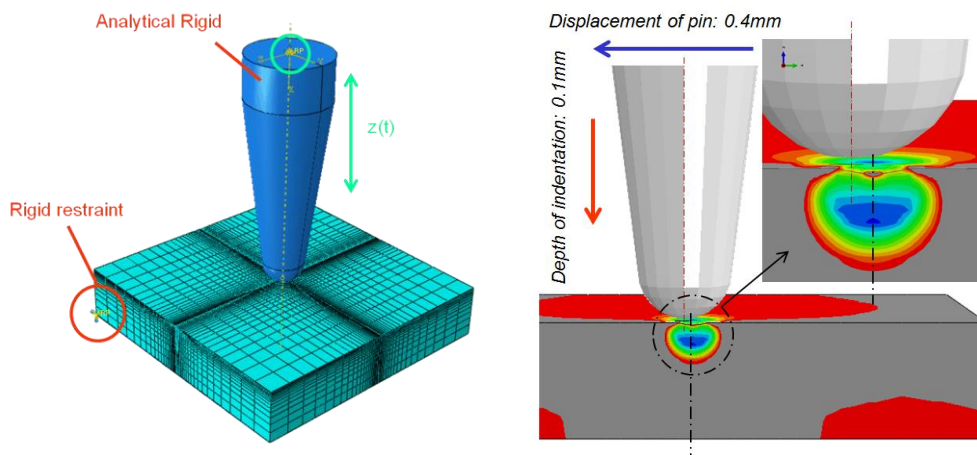


Fig. 14: Study of overlapping indentations [6]

Different movements of the pin are investigated to determine a sufficient numerical overlap of the individual pin indentations. It was found that a step displacement of 0.4 mm shows a good compromise between numerical calculation efforts and achieved three-dimensional geometry. This leads to at least five overlapping indentations for the contact area of the loaded pin. The remaining negligible geometric ripples were similarly observed in the real HFMI application.

Due to the impact of the indenter the elastic-plastic material undergoes a local hardened cycle. In structural weld simulation an isotropic hardening model is often used for a better matching of the residual stress distribution in welded structures made of construction steel [8]. But for high-strength steels, it is important to take advanced material properties like transformation plasticity [9] or application of phase-dependent hardening laws into account [10]. To study the effect of the hardening law on the stress-strain relationship, a single element was cyclic loaded. Fig. 15 compares an isotropic hardening law with a mixed isotropic-kinematic hardening model [11].

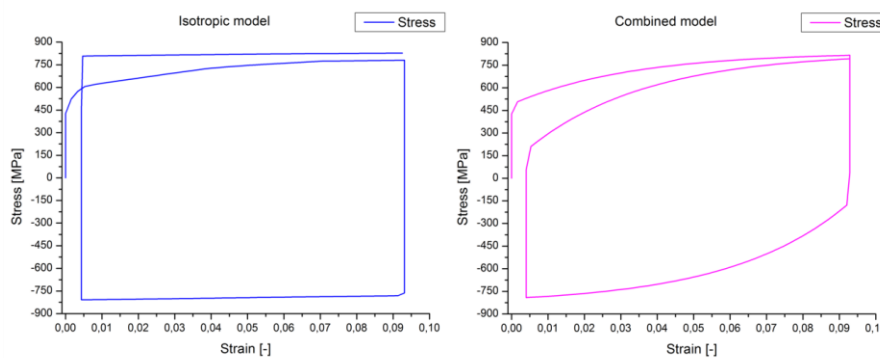


Fig. 15: Comparison of isotropic and isotropic/kinematic hardening [6]

The combined hardening model includes softening of material after change of loading direction and shows a sufficient matching hardening behaviour for the mild construction steel S355. In [12], the combined Chaboche-model implemented in *Abaqus*® is used for the simulation of the HFMI-treatment of austenitic and duplex stainless steels.

Last, the effect of a single pin indentation step or multiple incremental steps is investigated. Fig. 16 depicts the residual stress in loading direction for the single or incremental step movement applying the combined hardening law implemented in the structural finite element suite *Abaqus*®.

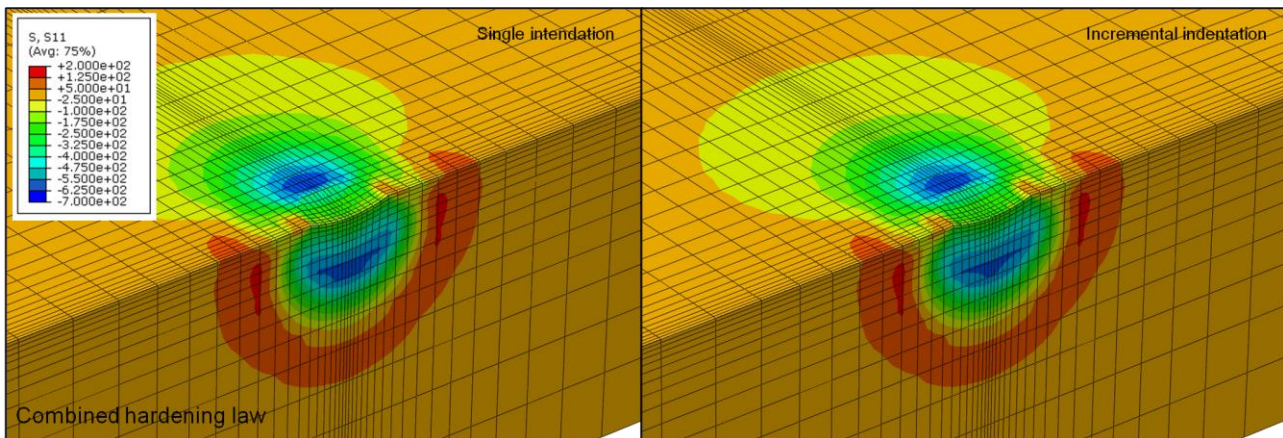


Fig. 16: Effect of single or incremental pin indentation on residual stress distribution [6]

If the indentation is applied in a single continuous movement of the pin, the influence of the hardening law is negligible. Maximum compressive stresses of 570 MPa are determined. According to the Hertzian contact between the globular tip of the pin and the plane plate, the maximum compressive stress is evaluated in a depth of 0.95 mm . If the same indentation depth is applied in five incremental steps, the maximum observed compressive stresses are marginally reduced to a value 560 MPa . More significant is that the size and location of the most stressed region changes to a smaller volume and gets closer to the surface. The maximum stress is evaluated at a depth of 0.75 mm .

For the subsequent time-consuming structural elastic-plastic simulation of the HFMI-treatment using *Abaqus*®, the mixed hardening model and a single indentation movement of the pin is applied. Beside the single displacement controlled movement of the pin, an overlapping of neighbored indentation occurs during the numerical treatment along the whole weld path.

4.2.2 Simulation of HFMI-treatment for investigated butt joint

After structural welding simulation in *Sysweld*®, the results of the butt joint including the residual stress state, plastic strains and phase-dependent material cards are imported into *Abaqus*®. Although the amount of data of gained three-dimensional weld simulation is excessive, the simulation of the HFMI-treatment is applied onto the whole model to avoid errors due to two-dimensional plane strain simplifications as discussed in [13]. The pin is modelled as rigid body with a tip radius of $r=2\text{ mm}$ and the specimen is clamped to the padding support. The indenter is adjusted at 75° to the top surface of the specimen, see Fig. 17. The applied axial travelling distance of the pin equals 0.1 mm , relating to the measured indentation of the micrographs. After each indentation the work piece is moved 0.4 mm along the weld path to achieve a sufficient overlapping of the impacts.

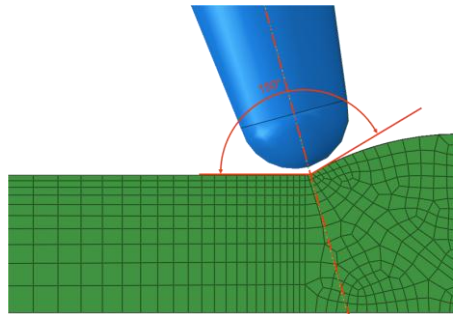


Fig. 17: Position and angle of rigid body pin [6]

Fig. 18 illustrates sequences of the HFMI-treatment process by the change of the residual stresses distribution. As expected, tensile residual stresses are reduced and the amount of compressive residual stresses in the weld toe increase due to the cyclic peening.

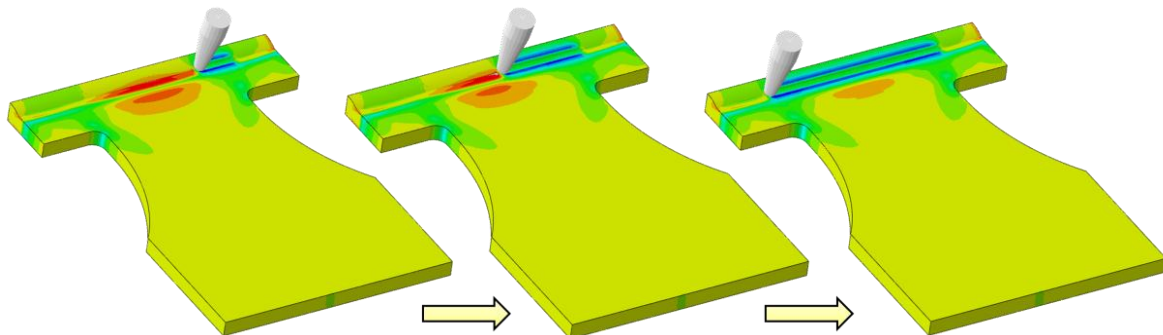


Fig. 18: Sequences during numerical HFMI process – transient stress distributions [6]

After the completed HFMI-treatment, the run-out plates are cut off. This causes minor stress redistribution at the lateral edges as shown in Fig. 19.

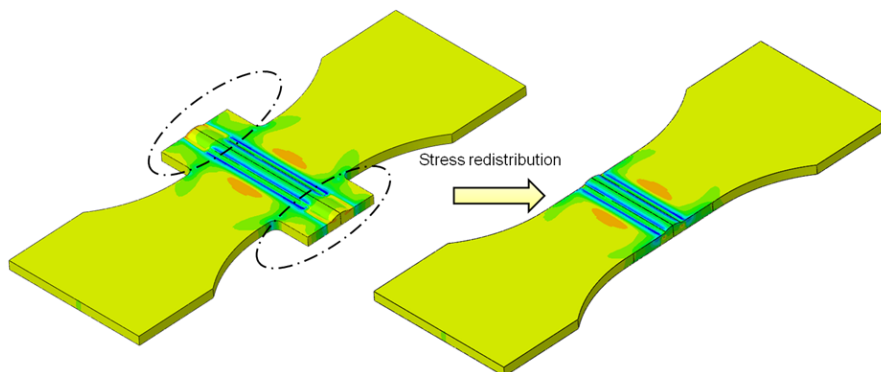


Fig. 19: Stress redistribution caused by removal of run out plates [6]

The cross-section distribution of residual stresses is shown in Fig. 20. At the top surface, compressive residual stresses appear into a depth of 1.5 mm , equilibrium conditions cause tensile residual stresses in the material depth below the treated volume.

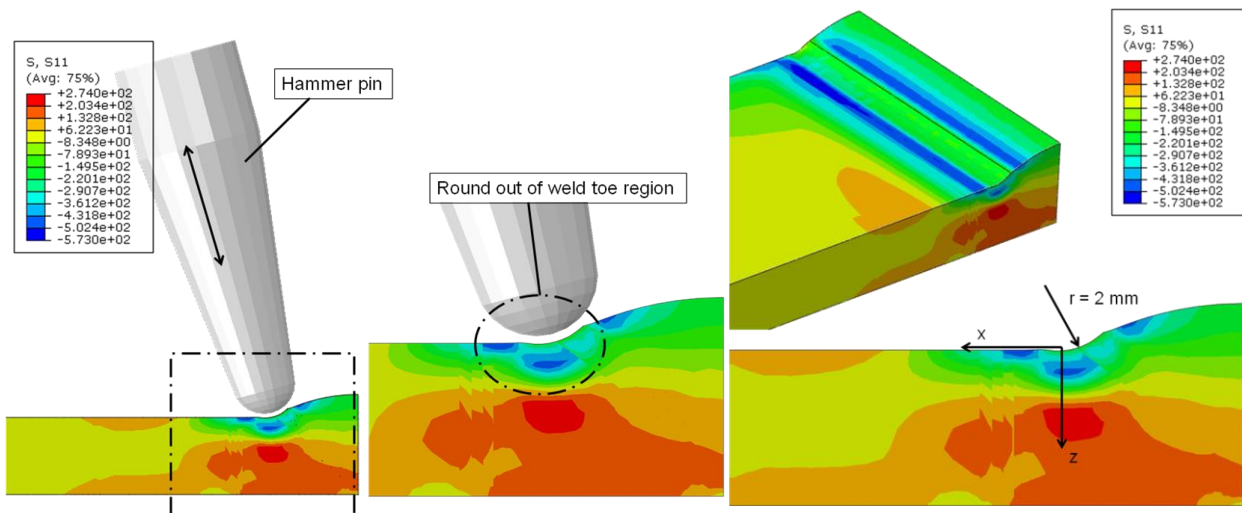


Fig. 20: Stress distribution and plastic deformation at the weld toe [6]

4.3 Local fatigue assessment

The local fatigue behaviour of HFMI-treated joints can be preferably evaluated by strain-based approaches due to the quite excessive elastic-plastic material condition in the treated weld toe region [14, 15].

In this work a stress based local fatigue approach is applied [16]. This assessment is based on the local stress gradient and takes the manufacturing induced residual stresses as external mean stresses into account. This superposition of manufacturing induced residual stresses and load based stresses leads to local plastic deformations if the material yield limit is exceeded. This plastic rearrangement deduces a subsequent change in the local mean stress as well as an amplitude correction using Neuber's stress-strain hyperbola.

A tumescent nominal tensile stress amplitude of 150 MPa is used as external load to determine the local fatigue at stress ratios of $R=0.1$ and $R=-1$. For each node a local S/N-curve is calculated by FemFat® based on nodal characteristics taking fatigue support, size effect, mean stress, statistical influence and surface roughness into account. The damage accumulation is done in accordance to Miner's law, modified by Haibach. Fig. 21 compares the local damage at a stress ratio of $R=0.1$ in the as-welded condition with the HFMI-treated solution incorporating the welding induced residual stresses in both cases.

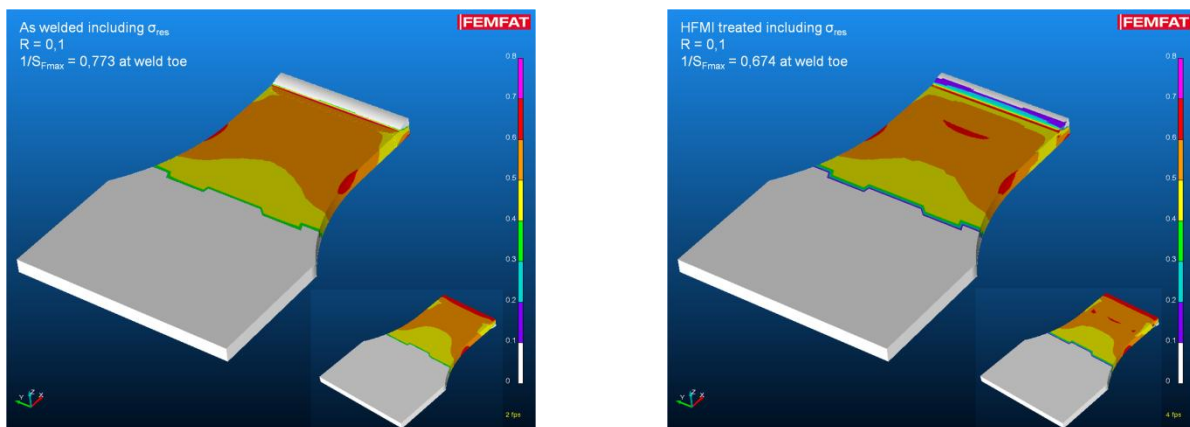


Fig. 21: Local fatigue assessment including residual stresses ($R=0.1$) [6]

The post-treated specimen shows a 13% reduced local damage at a stress ratio $R=0.1$ due to the decreased geometric notch effect and the superposition of compressive residual stresses by the HFMI-treatment. Fig. 22 exhibits the local fatigue life excluding the welding induced residual stresses. As expected, the results show a slightly higher local damage in both cases.

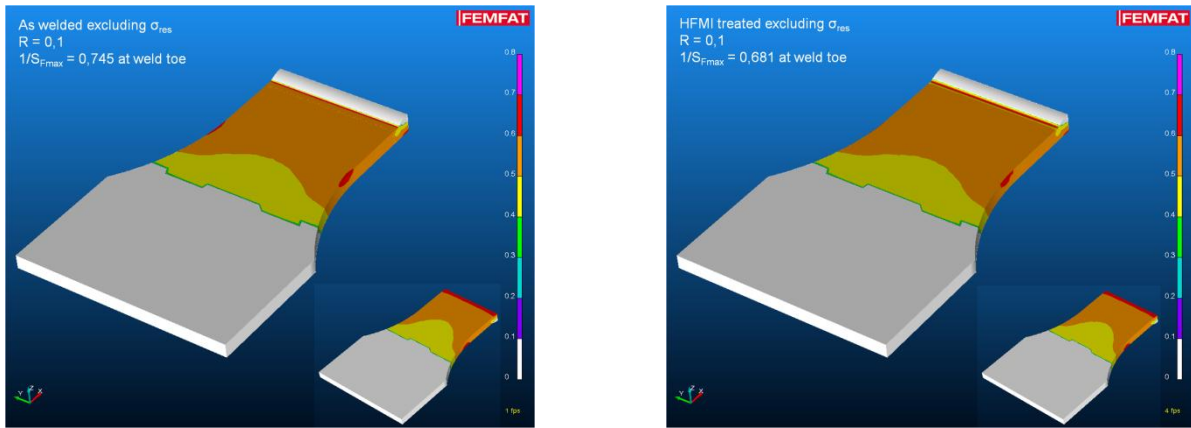


Fig. 22: Local fatigue assessment excluding residual stresses ($R=0.1$) [6]

The tabular results for two different stress ratios are shown in Fig. 23 and Fig. 24. It is shown that the effect of the shallower geometric notch is more important than the change towards compressive residual stresses by the HFMI-treatment. As the welding induced residual tensile stresses almost disappear in the HFMI-treated weld toe region for the investigated joint, it seems sufficient to take only the elastic-plastic HFMI-treatment without welding process induced residual stresses into account. This is recognizable by the minor change in damage sum of only one or two percent in the HFMI-treated condition by additional incorporation of the welding induced residual stress state.

Local damage ($R = -1$)	AW	HFMI
Including residual stresses σ_{res}	100%	83%
Excluding residual stresses σ_{res}	93%	85%

Fig. 23: Normalized improvement on fatigue life for $R=-1$

Local damage ($R = 0.1$)	AW	HFMI
Including residual stresses σ_{res}	100%	87%
Excluding residual stresses σ_{res}	96%	88%

Fig. 24: Normalized improvement on fatigue life for $R=0.1$

5 Conclusion

A three-dimensional closed simulation loop is built up, including a structural elastic-plastic weld simulation, a numerical computation of the HFMI process and stress-based fatigue life estimation. The welding simulation using *Sysweld*® takes phase-dependent material properties into account. Both the transient stress-strain results and the locally change in mechanical properties of the weld process are mapped to a structural elastic-plastic mechanical simulation.

An implicit, displacement controlled simulation of the HFMI-treatment was done using the software package *Abaqus*®. The applied indentation parameters of the moved pin base on measured values. The different elemental mechanical properties of the weld simulation were grouped into twelve material cards, whereat the elastic-plastic material behaviour was considered by a combined hardening model. Although high-performance-computing equipment was used, the computational time for the three-dimensional treatment is quite excessive. Summing up, the numerical HFMI-treatment results are in good accordance to measured values.

Finally, the fatigue life estimation based on local stresses showed the basic applicability of the simulation loop for the investigated thin-walled butt joint. A comparative study of the local damage sum revealed that HFMI-fatigue improvement due to the shallower geometric notch is more important than the beneficial effect of compressive residual stresses.

6 Outlook

Further investigations will include lifetime estimation of a HFMI-treated T-joint, compare to Fig. 25. Based on the presented simulation loop, a parametric study of the HFMI-treatment parameters on local fatigue life is scheduled. To improve the accuracy of the results, additional material parameters adjustment is also intended, especially in the case of numerical simulation of welded high-strength steel joints with subsequent HFMI-treatment and dynamical loading.

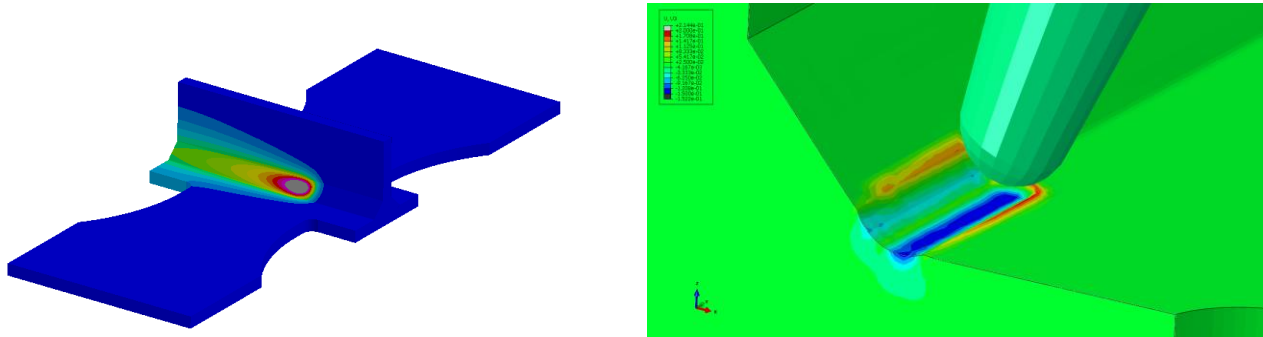


Fig. 25: Structural weld simulation and HFMI post-treatment in case of a T-joint

Acknowledgements

Financial support by the Austrian Federal Government (in particular from Bundesministerium für Verkehr, Innovation und Technologie and Bundesministerium für Wirtschaft, Familie und Jugend) represented by Österreichische Forschungsförderungsgesellschaft mbH and the Styrian and the Tyrolean Provincial Government, represented by Steirische Wirtschaftsförderungsgesellschaft mbH and Standortagentur Tirol, within the framework of the COMET Funding Programme is gratefully acknowledged.

REFERENCES

- [1] H.C. Yildirim, G.B. Marquis and Z. Barsoum: „Fatigue assessment of high frequency mechanical impact (HFMI)-improved fillet welds by local approaches“, *International Journal of Fatigue*, 52, 2013, pp. 57-67.
- [2] H.P. Günther, U. Kuhlmann: "Nachweiskonzepte zur Bemessung ermüdungsbeanspruchter Bauteile unter Berücksichtigung von Schweißnahtnachbehandlungsverfahren durch höherfrequenten Hämmern", *Stahlbau*, 78 (9), 2009, S. 613-621.
- [3] M. Leitner, M. Stoschka and W. Eichlseder: "Fatigue enhancement of thin-walled, high-strength steel joints by high frequency mechanical impact treatment", *Welding in the World*, 2013 (in review).
- [4] A. Hobbacher: "IIW Recommendations for Fatigue Design of Welded Joints and Components", *WRC Bulletin 520*, The Welding Research Council, New York, 2009.
- [5] M. Stoschka, M. Leitner and G. Posch: "Effect of high-strength filler metals on the fatigue behaviour of butt joints", *Welding in the World*, 57 (1), 2013, pp. 85-96.
- [6] D. Simunek: "Implementierung der Schweißnahtnachbehandlung mittels eines hochfrequenten Hämmerverfahrens in die numerische Lebensdauerabschätzung", Diploma thesis in progress, Montanuniversität Leoben, Chair of Mechanical Engineering, 2013 (in german).
- [7] C. Heinze, C. Schwenk and M. Rethmeier: „Influence of mesh density and transformation behaviour on the result quality of numerical calculation of welding induced distortion“, *Simulation Modelling Practice and Theory*, 19 (9), 2011, pp. 1847-1859.

- [8] T. Loose, J. Sakkietitbutra and J. Wohlfahrt: "New 3D-calculation of residual stresses consistent with measured results of the IIW round robin programme", *IIW Kenneth Easterling Best Paper Award*, 2009.
- [9] O. Muransky, C. Hamelin, M. Smith, P. Bendeich and L. Edwards: "The effect of plasticity theory on predicted residual stress fields in numerical weld analyses", *Computational Materials Science*, 54, 2012, pp. 125-134.
- [10] M. Ottersböck, M. Stoschka and M. Thaler: "Study of kinematic strain hardening law in transient welding simulation", *Mathematical Modelling of Weld Phenomena*, 10, 2013.
- [11] J.-L. Chaboche: "A review of some plasticity and viscoplastic constitutive theories", *International Journal of Plasticity*, 24, 2008, pp. 1642-1693.
- [12] R. Baptista, V. Infante and C. Branco: "Fully dynamic numerical simulation of the hammer peening fatigue life improvement technique", *Procedia Engineering*, 10, 2011, pp. 1943-1948.
- [13] M. Rahmann, N. Enzinger and C. Sommitsch: "Deformation and distortion induced by pneumatic impact treatment (PIT) in a welded joint for HS steel", *Proceedings of the International Workshop on Thermal Forming and Welding Distortion*, Bremen, April 6th-7th, 2011, pp. 203-213.
- [14] G. Le Quilliec, H.-P. Lieurade, M. Bousseau, M. Drissi-Habti, G. Inglebert, P. Macquet and J. Jubin: "Fatigue behaviour of welded joints treated by high frequency hammer peening: part II, numerical study", *International Institute of Welding*, Paris, IIW Document XIII-2395-11, 2011.
- [15] P. Schaumann and C. Keindorf: "Experiments and simulation of welded joints with post weld treatment", *Conference Proceedings of the International Conference on Welded Structures*, Miskolc, April 24th-26th, 2008.
- [16] W. Eichseder and B. Unger: "Prediction of the fatigue life with the finite element method", *SAE Paper 940245*, 1994.